ELSEVIER

Journal of Alloys and Compounds 356–357 (2003) 300–304

Journal of ALLOYS AND COMPOUNDS

www.elsevier.com/locate/jallcom

Refraction-like behaviour of hydrogen diffusion fronts

A. Remhof*, R.J. Wijngaarden, R. Griessen

Faculty of Sciences, Division of Physics and Astronomy, Vrije Universiteit De Boelelaan 1081, 1081 HV Amsterdam, The Netherlands

Received 10 June 2002; accepted 25 October 2002

Abstract

The local control of hydrogen mobility in thin films in combination with an optical indicator which exhibits hydrogen concentration dependent colors allows to visualize hydrogen diffusion in solids. The large mobility of hydrogen in metals and the possibility to tune it over several orders of magnitude makes thin film metal hydrides ideal systems. Planar structures such as prisms can be achieved, allowing to investigate the response of hydrogen diffusion fronts as they encounter these structures. Evidence for refraction-like phenomena at interfaces separating areas of different effective diffusivities are presented. The behaviour of the diffusion front can be described by a modified Snell's law, where the square root of the front mobility in the respective media plays the role of the refractive index.

Keywords: Hydrogen diffusion; Refraction of diffusion fronts; Optical hydrogen indication; Thin film hydrides

1. Introduction

The large mobility of hydrogen in metals [1] make metal hydrides ideal systems to investigate diffusion fronts in solids. The diffusion coefficient, characterizing the mobility of the diffusing particles, plays then a role analogous to the refractive index in classical optics. Unlike classical optics, where refractive index ratios of the order of 1 to 10 can be reached, for hydrogen diffusion the diffusion constants may be varied by many orders of magnitude at room temperature e.g. between 10^{-12} $cm^2\,s^{-1}$ for H in yttrium and 10^{-5} $cm^2\,s^{-1}$ for H in vanadium.

Recently, we demonstrated that a thin Y coating can be used as an optical indicator to visualize hydrogen migration in opaque vanadium films. The indicator method is a further development of the optical method presented by Den Broeder et al. [2] to monitor the *lateral* migration of hydrogen in Y, exploiting the intrinsic concentration dependent optical properties of the YH system [3]. Thus spatial and temporal concentration variations within a Y–H_x film can easily be monitored optically. Especially the diffusion front separating the coexisting α- and β-phases is clearly identified as a discontinuous change in transmission and reflection. In Y the phase boundary of the *hcp* α-phase is $c_{\alpha,max} = 0.2$ H/Y and that of the *fcc* β-phase is $c_{\beta,min} = 1.9$ H/Y, thus $\Delta c = c_{\beta,min} - c_{\alpha,max} = 1.7$ H/Y [4,5]. The indicator technique makes use of the fact that: (i) the H-diffusion coefficient in V is orders of magnitude higher than the one in Y and (ii) the hydrogen affinity of V is low compared to the hydrogen affinity of Y. Consequently H migrates mainly via the V layer to the Y indicator. As the total H flux through a sample scales with its cross section, a thick V film can supply more H to the Y indicator layer than a thin one. On the other hand, a thicker indicator layer requires larger quantities of H to change its optical appearance. Thus, the effective H mobility can be tuned via the V/Y thickness ratio. Using shadow masks during deposition, it is possible to vary the V/Y thickness ratio locally and to create for example, single thickness steps or more complex planar structures such as 'prisms'.

Previously, the reflection-like behaviour of diffusional *waves* has been studied on diffusive photon waves in turbid media [6]. We extend these studies to the diffusion of hydrogen in metals. We present direct observation of diffusion *fronts* in solid-state diffusion and examine how these fronts propagate from one medium into another. Our results suggest that the concept of a diffusional index of refraction can also be applied to solid-state diffusion and that a diffusion front crossing an interface obeys a modified Snell's law.

*Corresponding author. Present address: Institut für Experimentalphysik, Ruhr-Universität Bochum, D-44780 Bochum, Germany.

E-mail address: arndt.remhof@ruhr-uni-bochum.de (A. Remhof).

0925-8388/02/$ – see front matter
doi:10.1016/S0925-8388(02)01274-4

2. Sample preparation and experimental details

The samples are prepared by means of e-gun evaporation in an ultra high vacuum system (background pressure $< 10^{-9}$ mbar). A typical sample consists of a V layer deposited at a rate of 0.05 nm s^{-1} onto a polished amorphous quartz substrate (Suprasil 1, Heraeus), kept at room temperature. With the help of shadow masks we vary locally the thickness of the layer and thereby create V patterns as single thickness steps or more complex planar structures such as triangles. Subsequently, the V film is covered with a 50 nm thick Y layer, serving later on as the optical indicator for hydrogen diffusion. Finally, to enable hydrogen uptake the samples are partially covered with a 10 to 15 nm thick Pd layer, deposited under the same conditions. Again shadow masks allow to pattern the Pd cover layer. Usually, single Pd dots of 500 μm or Pd stripes with a typical width of 1–2 mm are used. In ambient air the uncovered parts of the sample oxidize superficially. This natural oxide layer prevents the sample from further corrosion and blocks hydrogenation. The deposition process (thickness, growth rate) of the metallic layers is monitored in situ by means of a water cooled quartz microbalance. Prior to hydrogenation the sample thickness is measured ex situ by profilometry and by Rutherford backscattering (RBS). Furthermore, RBS is used to check for chemical impurities and to detect eventual alloy formation at the interfaces. The RBS spectra show well defined layers, no intermixing at the interfaces and no chemical contaminations. The thickness of the natural oxide layer formed in ambient air on the uncovered part of the yttrium layer is determined to be 15 nm.

In this work we discuss two different samples. Schematic sample designs are displayed in Fig. 1. First (Fig. 1a) the analogon to an optical prism is constructed as follows: We deposit a 150 nm thick triangular V island on top of a 75 nm thick V layer prior to the Y coating. The thickness of 75 nm is thin enough to investigate the optical response of the Y indicator layer in transmission as well as in reflection. The V triangle is right-angled, the relevant angle being 8 degrees. The Pd stripe which serves as a H inlet is finally evaporated parallel to the long cathetus. The distance between the Pd stripe and the triangle is 440 μm. This sample is intended for the study of the 'refraction' of a straight diffusion front encountering the interfaces separating regions of different effective H diffusivity. Second (Fig. 1b) we prepare a V film with a single thickness step. One half of the 10×10 mm^2 substrate is covered with a 50 nm thick V layer while the other half is covered with a 250 nm thick V layer. Subsequently the whole sample is covered with a 50 nm thick Y layer. Finally a circular Pd dot (0.5 mm in diameter, 10 nm in thickness) is deposited on the thinner side of the sample, 1.5 mm away from the interface. This sample is intended for a study of the 'refraction' of a curved (circular) diffusion front as it encounters the interface.

The hydrogen gas loading is carried out in a gas-tight stainless steel cell, equipped with a gas handling system, temperature control and optical windows. The gas loading cell is mounted onto the positioning table of an optical microscope (Olympus BX60F5). Illuminated by white lamps, changes in the optical appearance are monitored by means of a three-CCD red–green–blue (RGB) colour camera (Sony DXC–g50P). This camera possesses CCD chips with arrays of 582 by 782 pixels. For the small magnifications used in this study, the spatial resolution of 2×2 μm^2 is determined by the pixel size of the camera.

3. Results and discussion

Fig. 2 shows a sequence of the H loading of the first sample, the 'prism'. All four images depict a 3.2×1.6 mm^2 large area of the sample. The images are recorded in a combined reflection and transmission mode, the initial color pictures have been transformed into a gray scale. The thicker part of the V film (the 'prism') can be identified as the dark, triangular shaped object. The Pd stripe, serving as H inlet, covers the bottom part of the pictures. At $t = 0$ the sample is exposed to a hydrogen atmosphere at 1 bar.

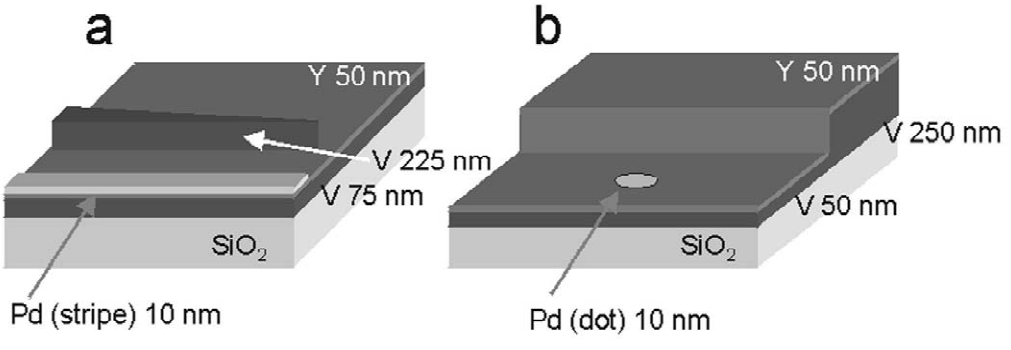

Fig. 1. Schematic sample design. Patterned V films on SiO_2 substrates, covered with 50 nm Y. To enable H loading, Pd inlets were deposited on top of the samples. In ambient air the Pd-free parts of the samples will oxidize superficially. Sample a consists of a 150 nm thick triangular V island on top of a 75 nm thick V layer. H enters via a 10 nm thick Pd stripe, 0.44 mm away from the triangle. The V layer of sample 'b' has a 200 nm high step. The Pd inlet is a circular dot (diameter 0.43 mm) deposited 1.34 mm away from the interface on the thinner side.

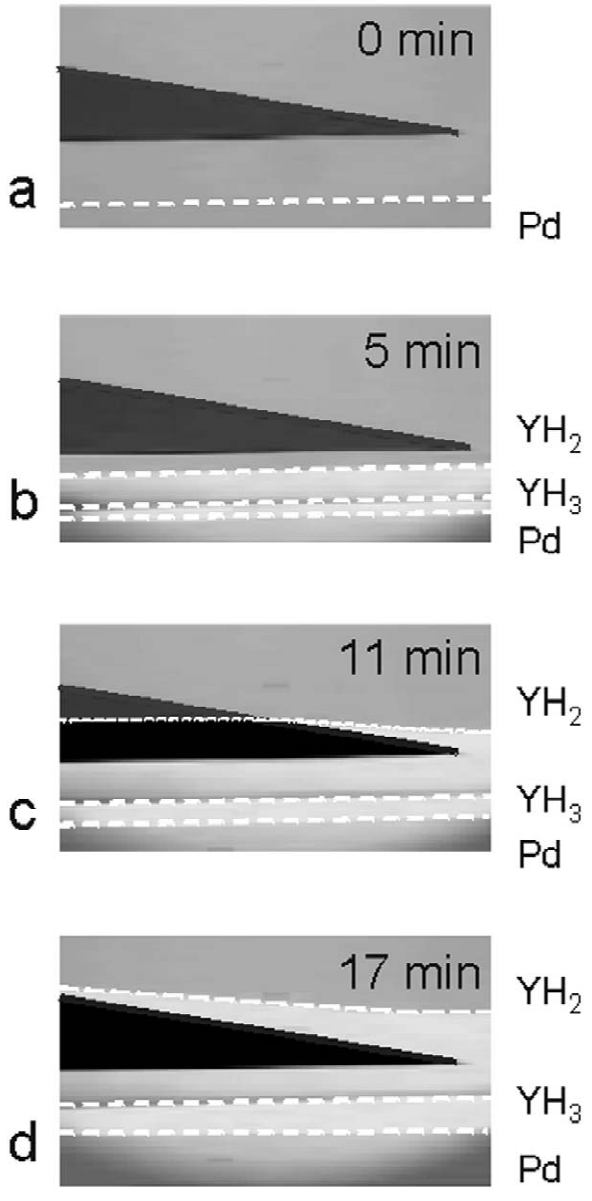

Fig. 2. Evolution of the diffusion fronts in sample 'a'. All images depict a 3.2×1.6 mm^2 large area of the sample. The 150 nm thick triangular V island appears as the dark object dominating the photographs. The Pd stripe, serving as H inlet, covers the bottom part of the pictures. With increasing time the hydride fronts progress into the sample, away from the Pd inlet. The refraction-like behaviour of the 'V-prism' is clearly visible. The respective interfaces are highlighted by dashed lines for clarity.

During the whole experiment the temperature is kept constant at 373 K. The other images are recorded at $t = 5$, $t = 11$ and $t = 17$ min, respectively. The Y underneath the Pd stripe immediately starts absorbing hydrogen and forms the yellowish transparent $YH_{3-\delta}$ phase. Further hydrogen uptake leads to lateral hydrogen diffusion away from the Pd covered part of the sample. The H concentration in the indicator layer decreases from $c_H = 2.7$ H/Y in the trihydride phase below the Pd to essentially $c_H = 0$ far from it. The large miscibility gaps, separating the stable hydride phases in the Y–H system cause a discontinuous concentration profile in the sample. As each of the hydride phases exhibits characteristic optical properties, it can be easily distinguished by its optical appearance. The front separating the opaque α- from the reddish β-phase as well as the front between the reddish β- from the bright, yellowish transparent γ-phase can be identified as discontinuous changes in optical contrast, both in reflection and in transmission. For clarity, we marked the respective diffusion fronts as well as the Pd border by dashed lines. The progression of the hydride fronts with time is clearly visible. As YH_2 appears darker in reflection than the pure shiny metal, the front between YH_2 and Y can also be seen as it crosses the opaque V triangle (Fig. 2c). Note the H concentration dependent transmission in YH_2. Within YH_2 the transmission decreases with increasing c_H. Therefore, in transmission, YH_2 appears more bright in contact with the (almost) H free metal than close to the hydrogen rich YH_3-phase.

Here we restrict ourselves to the description and discussion of the front separating the opaque α- from the reddish β-phase. In the following we call this optical feature simply *the front*. It progresses with a mobility $K_1 = 6\times10^{-6}$ cm^2 s^{-1}, which agrees nicely with the behaviour of Y/V bilayers under the same conditions [7]. As soon as the front reaches the triangle its mobility increases to $K_2 = 1.7\times10^{-5}$ cm^2 s^{-1}. While the front moves through the V triangle, it stays parallel to the Pd border, making an angle of $\theta_2 = 8°$ with the second interface (the hypotenuse of the triangle). The front leaves the V triangle under an angle of $\theta_1 = 4.5°$. Experimentally we find

$$\frac{\sin\theta_1}{\sin\theta_2} = \frac{v_{f1}}{v_{f2}} = \frac{\sqrt{K_1}}{\sqrt{K_1}}, \quad (1)$$

where v_{f1} denotes the *momentary* velocity of the front just before it reaches the interface at a given point and v_{f2} its *momentary* velocity just after passing the interface at the same point. Eq. (1) reminds us of the refraction of an optical wave front (i.e. a constant phase surface) by an optical prism. In optics, refraction is caused by the speed of light being different in the two different media. It is described by Snell's law: $n_2/n_1 = \sin\theta_1/\sin\theta_2$, where $\theta_{1,2}$ are the enclosed angles of the incoming and refracted beam with the interface normal. The media on either side of the interface separating them are characterized by their respective refractive indices n_1 and n_2. The refractive index of a given medium is defined as the ratio of the speed of light in vacuum to the speed of light in this medium. In our case of diffusion, each of the individual diffusing H-atoms undergoes a random walk, driven by the concentration gradient, resulting in a monotonously decreasing velocity of the front. In a homogeneous medium, the front progresses as $x_f = \sqrt{Kt}$, leading to a front velocity of $v_f = dx_f/dt = 1/2\sqrt{K/t}$. In our experiment the velocity ratio coincides with the ratio of the square roots of the respective front mobility in the two media.

In a second experiment, we generate circular fronts and monitor their behaviour as they cross a straight interface, separating two different media whose effective diffusivities differ by a factor of 4.5. The Pd dot (0.43 mm diameter), serving as the H inlet, is placed on top of the low-diffusivity medium, 1.34 mm away from the interface. Under the same loading conditions as before, the evolving phase boundaries form circular rings that expand with time. Again we observe a behaviour as the radius of the outer ring progresses as $r = \sqrt{K_1 t}$ where $K_1 = 4.1 \times 10^{-6}$ $cm^2\,s^{-1}$. As soon as the front reaches the high diffusivity medium the front bulges out and a mushroom shaped pattern is formed. Fig. 3 depicts the situation 216 min after the sample was exposed to a H atmosphere of 1 bar at 373 K. On top of the photograph, which displays a 4.5×5.6 mm^2 area of the sample, we construct four 'rays' to demonstrate Snell's law. A 'ray' originating at the center of the Pd dot intersects the interface normal with an angle θ_1. The refracted ray is constructed in such a way that it starts at the intersection point and crosses perpendiculary the diffusion front in the fast medium. It makes an angle θ_2 with respect to the interface normal. Within the accuracy of the experiment Snell's law $\sin\theta_2 / \sin\theta_1 = \sqrt{K_2}/\sqrt{K_1} = 2.1$ accurately describes the refraction of the diffusion front. The 'refracted' diffusion front becomes distorted as $\sin\theta_2$ approaches unity. A somewhat similar distortion has been observed by O'Leary et al. for the refraction-like behaviour of photon density waves in turbid media. Our experiment has the advantage over O'Leary et al.'s experiment, that we can observe the full pattern, including the distorted area close to the interface.

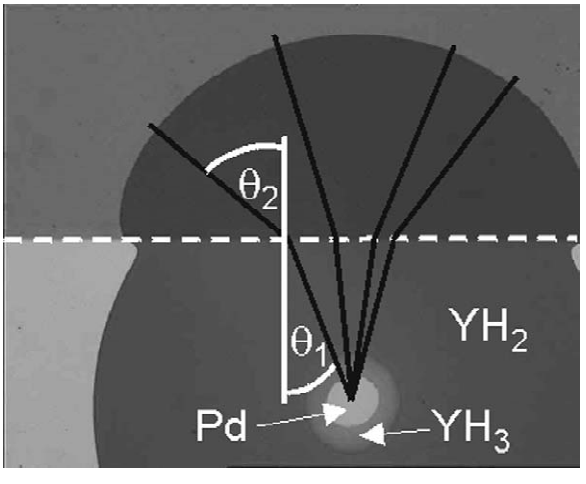

Fig. 3. Hydrogen diffusion front in sample 'b'. The image depict a 5.6×4.5 mm^2 large area of the sample. The image is recorded in reflection, 216 min after the sample was exposed to a H atmosphere of 1 bar at 373 K. The initially circular shaped diffusion front gets distorted as it crosses the interface separating two areas of different effective diffusivities. The mushroom-shaped pattern can be explained by a modified Snell's law, where $\sqrt{K}$ plays the role of the index of refraction.

4. Summary and outlook

We demonstrate that the local control of hydrogen mobility in thin films in combination with an optical indicator, which exhibits hydrogen concentration dependent colors, allows for a real time study of solid state diffusion (in our case of hydrogen in metals). In thin films planar structures as interfaces and 'prisms' can be achieved, and makes it possible to investigate the behaviour of hydrogen diffusion fronts as they encounter these structures. Like light in turbid media diffusing H fronts obey a modified Snell's law, where the square root of the front mobilities in the respective media take the place of the refraction index. Though the observed similarities with classical optical phenomena are striking, the deviation from Snell's law at large angles show that the analogy is poor. Mandelis et al. [11] showed, that refraction-like and reflection-like behaviour can be derived from interfacial flux expressions. Their calculations yield Snell's law as an adequate approximation under near-normal incidence.

Future investigations will include hydrogen electro-diffusion waves. Ordinary diffusion waves arise from forced oscillations of diffusing particles. Denoting the particle density as c and the diffusivity as D, diffusion waves are mathematically described as solutions of the diffusion equation

$$\frac{\partial c}{\partial t} = D\,\Delta c, \tag{2}$$

in which $c(\vec{r},\ t)$ varies as $c(0,t) = \sin(\omega t)$ at the origin. Examples are oscillating temperature such as the temperature profile of the earth resulting from the seasonal temperature variation [8] or diffuse photon density waves in a turbid medium [6]. Reviews on diffusion waves together with examples of their technological applications have been published by Yodh [9] and by Mandelis [10]. Diffusion waves are heavily damped, so that the wave can only be observed over one wavelength. That makes experimental studies difficult. One-way to overcome this problem are *electro-diffusion waves*. In the presence of a constant electric field $\vec{E}$ a charged particle experiences an additional force, leading to electro-diffusion waves that are solutions of a modified diffusion equation [12]:

$$\frac{\partial c}{\partial t} = D\,\Delta c - \frac{\mathrm{d}}{\mathrm{d}c}\left[\frac{eZD}{\partial\mu/\partial c}\right]\left(\vec{E}\cdot\vec{\nabla}c\right), \tag{3}$$

where eZ denotes the effective charge of the particle, and μ is the chemical potential of H in the metal. The prefactor of the linear term of Eq. (3).

$$v(c) = \frac{\mathrm{d}}{\mathrm{d}c}\left[\frac{eZD}{\partial\mu/\partial c}\right]\vec{E} \tag{4}$$

has the dimension of a velocity. Electro-diffusion waves exist at all frequencies and suffer less from damping than ordinary diffusion waves. Electromigration studies on thin

film YH_x samples demonstrated that H in Y behaves like a negatively charged particle [2,12], opening the possibility to work with electro-diffusion waves.

To gain a deeper understanding of the observed phenomena we are presently carrying out numerical simulations in which the 2D diffusion equation is solved on a square lattice. The simulation program also allows to model diffusion waves. First results are promising. The mushroom-shaped front of Fig. 3 is nicely reproduced by the simulations.

Acknowledgements

We would like to thank N.J. Koeman for the careful preparation of the samples, L.C.J.R. Jansen and J.H. Rector for technical support as well as B. Dam and S.J. van der Molen for fruitful discussions. This work is part of the research program of the Stichting voor Fundamenteel Onderzoek (FOM) which is financially supported by the Dutch NWO.

References

[1] G. Alefeld, J. Völkl (Eds.), Hydrogen in Metals, Vols. 1 and 2, Springer Verlag, Berlin, 1978.
[2] F.J.A. den Broeder, S.J. van der Molen, M. Kremers, J.N. Huiberts, D.G. Nagengast, A.T.M. van Gogh, W.H. Huisman, N.J. Koeman, B. Dam, J.H. Rector, S. Plota, M. Haaksma, R.M.N. Hanzen, R.M. Jungblut, P.A. Duine, R. Griessen, Nature (London) 394 (1998) 656.
[3] M. Kremers, N.J. Koeman, R. Griessen, P.H.L. Notten, R. Tolboom, P.J. Kelly, P.A. Duine, Phys. Rev. B 57 (1998) 4943.
[4] P. Vaida, in: K.A. Gschneidner, L. Eyring (Eds.), Handbook on the Physics and Chemistry of Rare Earth, Vol. 20, Elsevier, Amsterdam, 1995.
[5] E.S. Kooij, A.T.M. van Gogh, R. Griessen, J. Electrochem. Soc. 146 (1999) 2990.
[6] M.A. O'Leary, D.A. Boas, B. Chance, A.G. Yodh, Phys. Rev. Lett. 69 (1992) 2658.
[7] A. Remhof, S.J. van der Molen, A. Antosik, A. Dobrowolska, N.J. Koeman, R. Griessen, Phys. Rev. B 66 (2002) R 020101.
[8] A. Sommerfeld, Partielle Differentialgleichungen der Physik (reprint of the 6th edition) (Verlag Harri Deutsch, Thun, 1978).
[9] A. Yodh, B. Chance, Phys. Today 48 (03/1995) 34.
[10] A. Mandelis, Phys. Today 53 (08/2000) 29, and references therein.
[11] A. Mandelis, L. Nicolaides, Y. Chen, Phys. Rev. Lett. 87 (2001) 020801.
[12] S.J. van der Molen, M.S. Welling, R. Griessen, Phys. Rev. Lett. 85 (2000) 3882.